Supporting Information for:

Correlation of methane activation and oxide catalyst reducibility and its implications for oxidative coupling

*Gaurav Kumar, Sai Lap Jacky Lau, Matthew D. Krcha, Michael J. Janik **

Department of Chemical Engineering, The Pennsylvania State University, University Park, PA

16802

mjanik@engr.psu.edu

Information available:

Table S1. Valence configurations for metal oxides with transition metal dopants

Table S2. *K-point* sampling with the third vector perpendicular to the surface, and the meshes used for the metal oxides

Table S3A. Lattice constants of the metal oxides

Table S3B. Surface facets, number of atomic layers, number of frozen layers, and the number of atoms in the surface slab for each metal oxide

Table S3C. Atomistic structures of bulk, and bare, oxygen vacant, H-adsorbed and $\cdot CH_3$ adsorbed surfaces of different metal oxides

Table S4. Values for Fermi energy, energy in the vacuum and work function

Table S5. Oxygen vacancy formation energy ΔE_{vac}, C-H activation reaction energy ΔE_{act}, $\cdot CH_3$ adsorption energy ΔE_{ads} of all the pure/doped oxides used in the universal correlation

Table S6. Statistical details of the correlation between C-H bond activation of methane ΔE_{act} and the oxygen vacancy formation energy ΔE_{vac}

Table S7. The position of oxygen vacancies in various stable oxidation states of TbO_x in a mirrored $Tb_{16}O_{32}$ surface slab

Table S1. Valence configurations for metal oxides with transition metal dopants

Metal Oxide	Dopant	Valence Configuration
CeO_2	Ag	$4d^{10}5s^{1}$
	Mn	$3d^{6}4s^{1}$
	Ni	$3d^{8}4s^{2}$
	Pd	$4d^{9}5s^{1}$
	Pt	$5d^{9}6s^{1}$
	V	$3d^{4}4s^{1}$
	W	$5d^{4}6s^{2}$
	Zn	$3d^{10}4p^{2}$
	Zr	$4s^{2}4p^{6}4d^{2}5s^{2}$

Metal Oxide	Dopant	Valence Configuration
MgO	Be	$2s^{2}$
	Cr	$3d^{5}4s^{1}$
	Cu	$3d^{10}4\mathrm{p}^{1}$
	Eu	$5s^{2}5p^{6}4f^{7}6s^{2}$
	Fe	$3d^{7}4s^{1}$
	Ga	$4s^{2}4p^{1}$
	Ge	$4s^{2}4p^{2}$
	In	$5s^{2}5p^{1}$
	Li	$1\mathrm{s}^{1}2\mathrm{s}^{1}2\mathrm{p}^{1}$
	Mn	$3d^{6}4s^{1}$
	Ni	$3d^{8}4s^{2}$
	Pd	$4d^{9}5s^{1}$

Metal Oxide	Dopant	Valence Configuration
TiO_2	Ce	$4s^{2}4p^{6}4f^{1}5d^{1}6s^{2}$
	Fe	$3\mathrm{p}^{6}3\mathrm{d}^{7}4\mathrm{s}^{1}$
	Zr	$4s^{2}4p^{6}4d^{2}5s^{2}$

Table S2. *K-point* sampling with the third vector perpendicular to the surface, and the meshes used for the metal oxides. For doped systems, similar *k-point* was used as the host oxide

Metal Oxide	*k-points*
Anatase TiO_2	3x3x1
CeO_2	2x2x1
MgO	3x3x1
Rutile TiO_2	3x3x1
TbO_x	2x2x1
ZnO	3x3x1

Table S3A. Lattice constants of the metal oxides

Metal Oxides	Lattice constants (in Å)
Anatase TiO_2	a = b = 3.789, c = 9.817
CeO_2	a = b = c = 5.481
MgO	a = b = c = 4.234
TbO_x	a = b = c = 5.449
Rutile TiO_2	a = b = 4.594, c = 2.959
ZnO	a = b = 3.283, c = 5.260

Table S3B. Surface facets, number of atomic layers, number of frozen layers, and the number of atoms in the surface slab for each metal oxide

Metal Oxides	Mirrored/ Non-mirrored	Surface facets	Number of atomic layers	Number of frozen layers	Number of atoms	
					Metal	Oxygen
Anatase TiO_2	Non-mirrored	100	4	0	16	32
Anatase TiO_2	Non-mirrored	101	2	0	16	32
Anatase TiO_2 (doped)	Non-mirrored	001	4	2	16	32
CeO_2 (pure/doped)	Mirrored	111	4	0	16	32
MgO	Mirrored	110	11	0	44	44
MgO	Non-mirrored	100	4	2	32	32
MgO (pure/doped)	Mirrored	100	5	1	40	40
Rutile TiO_2	Non-mirrored	110	3	0	24	48
TbO_x	Mirrored	111	4	0	16	16x
ZnO	Non-mirrored	001	5	0	40	40
ZnO	Non-mirrored	100	5	0	40	40
ZnO	Non-mirrored	110	5	0	40	40

Table S3C. Atomistic structures of bulk, and bare, oxygen vacant, H-adsorbed and $\cdot CH_3$ adsorbed surfaces of different metal oxides

Side views of bulk a) Anatase TiO_2, b) CeO_2, c) MgO, d) Rutile TiO_2, e) TbO_2, and f) ZnO. Ti is shown in grey, Ce in off white, Mg in bright green, Tb in turquoise, Zn in blueish grey, and O in red.

a 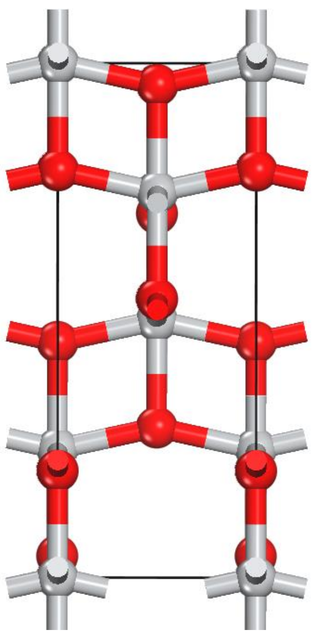	b 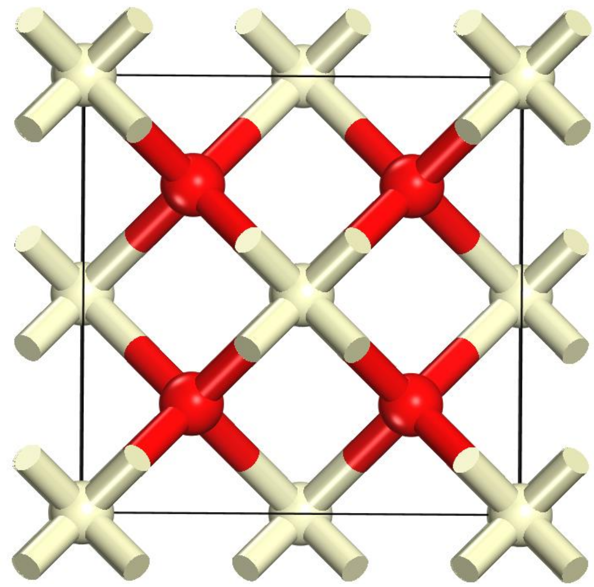
c 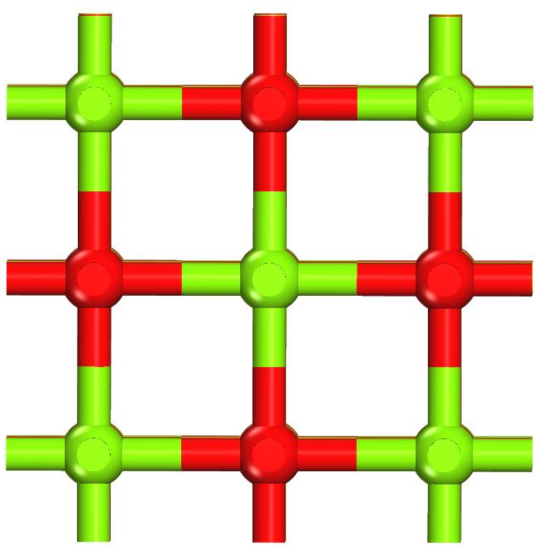	d 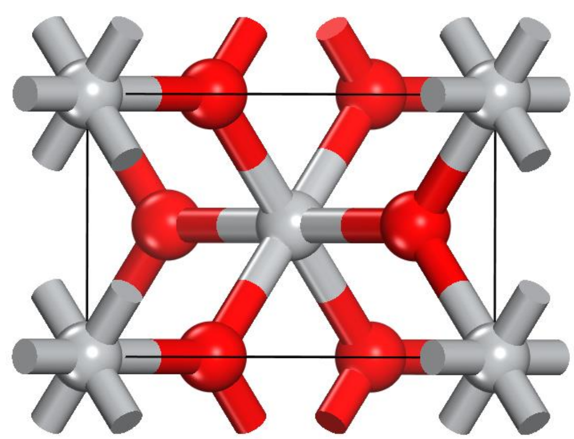

e

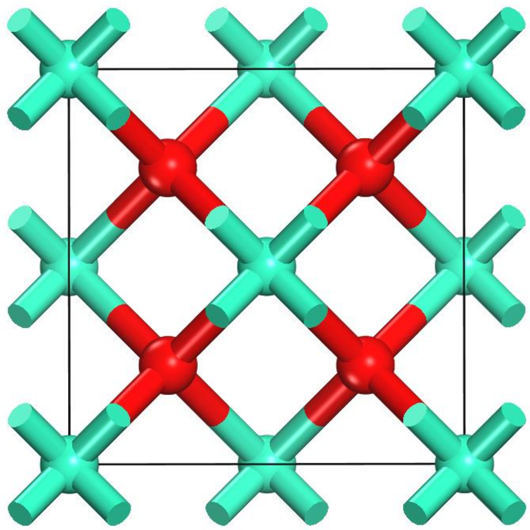

f

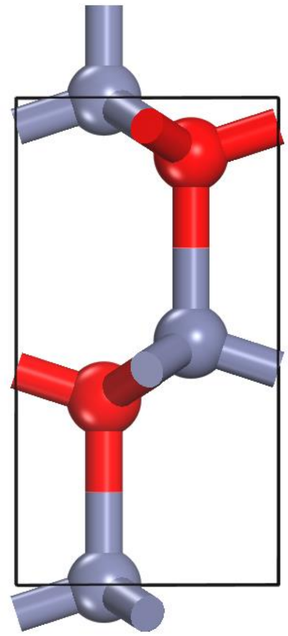

Side views of anatase TiO_2 (100) a) bare surface, b) oxygen vacant surface at the bridge (missing oxygen is shown as a dotted circle), with c) H adsorbed at the bridging oxygen, and d) $\cdot CH_3$ adsorbed at the bridging oxygen. Ti is shown in grey (light), O is shown in red (dark), C in dark grey, and H in white.

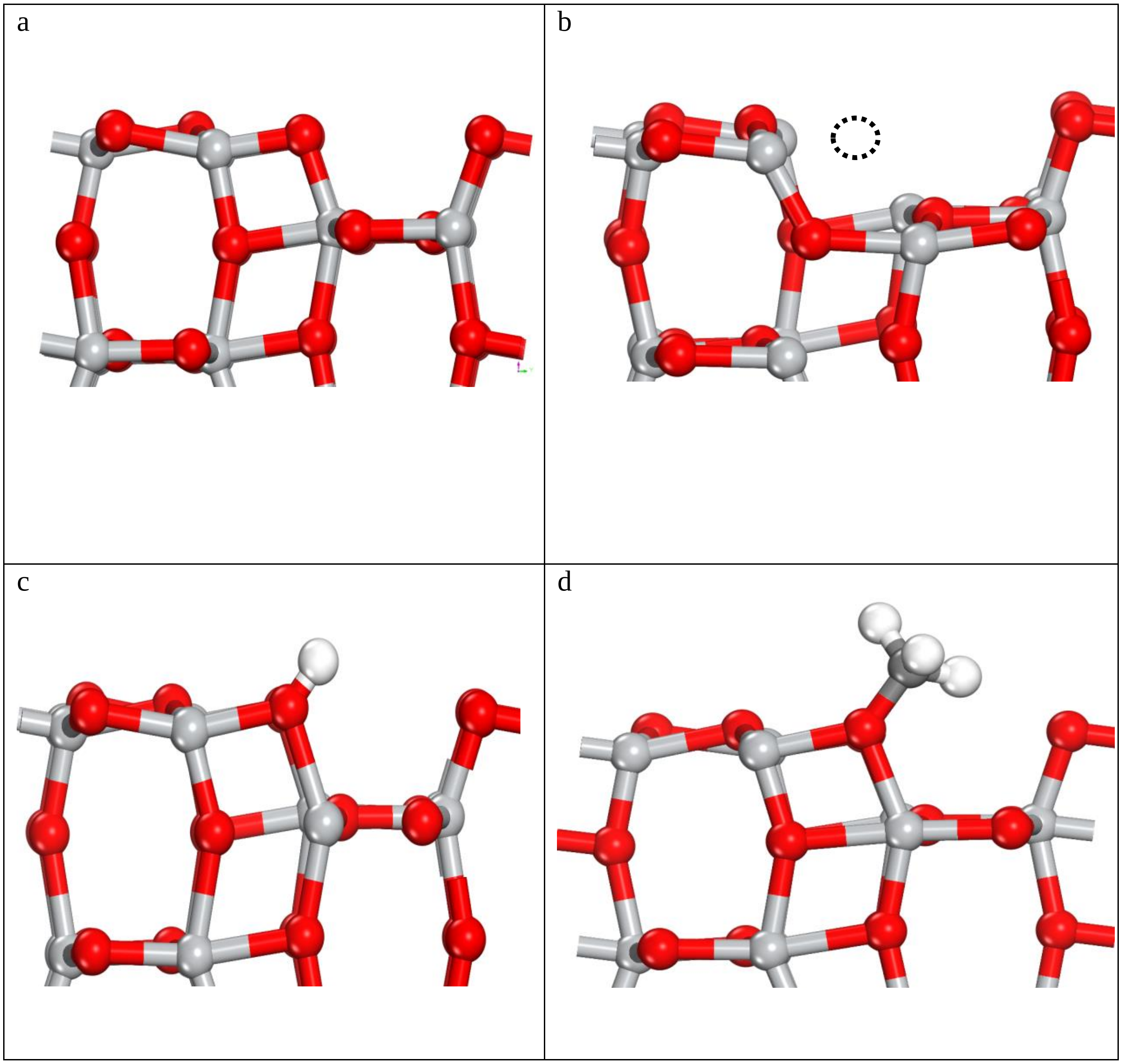

Side views of anatase TiO_2 (100) a) bare surface, b) oxygen vacant surface in plane (missing oxygen is shown as a dotted circle), with c) H adsorbed at the in-planed oxygen, and d) $\cdot CH_3$ adsorbed at the in-planed oxygen. Ti is shown in grey (light), O is shown in red (dark), C in dark grey, and H in white.

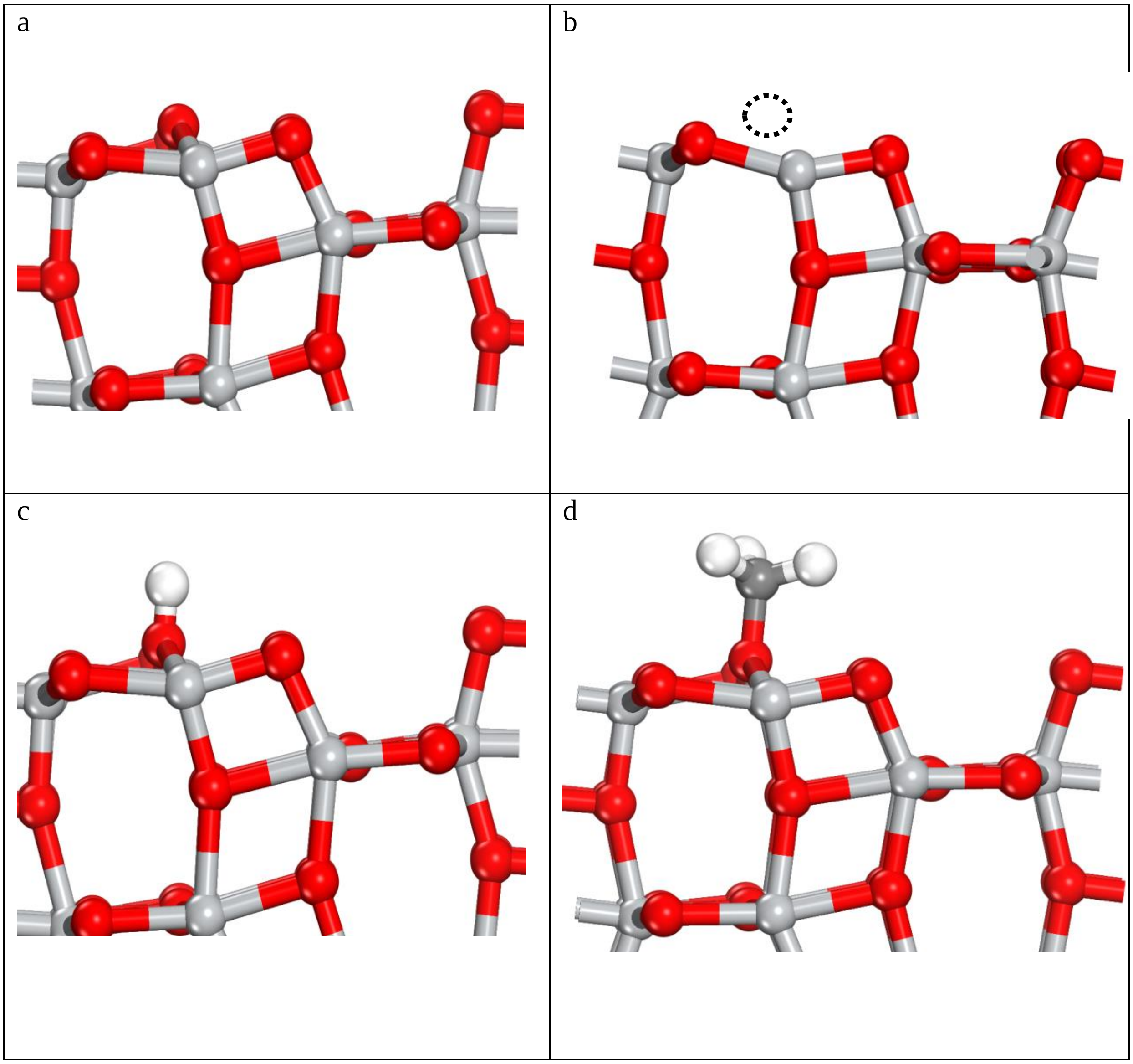

Side views of anatase TiO_2 (101) a) bare surface, b) oxygen vacant surface at the bridge (missing oxygen is shown as a dotted circle), with c) H adsorbed at the bridging oxygen, and d) $\cdot CH_3$ adsorbed at the bridging oxygen. Ti is shown in grey (light), O is shown in red (dark), C in dark grey, and H in white.

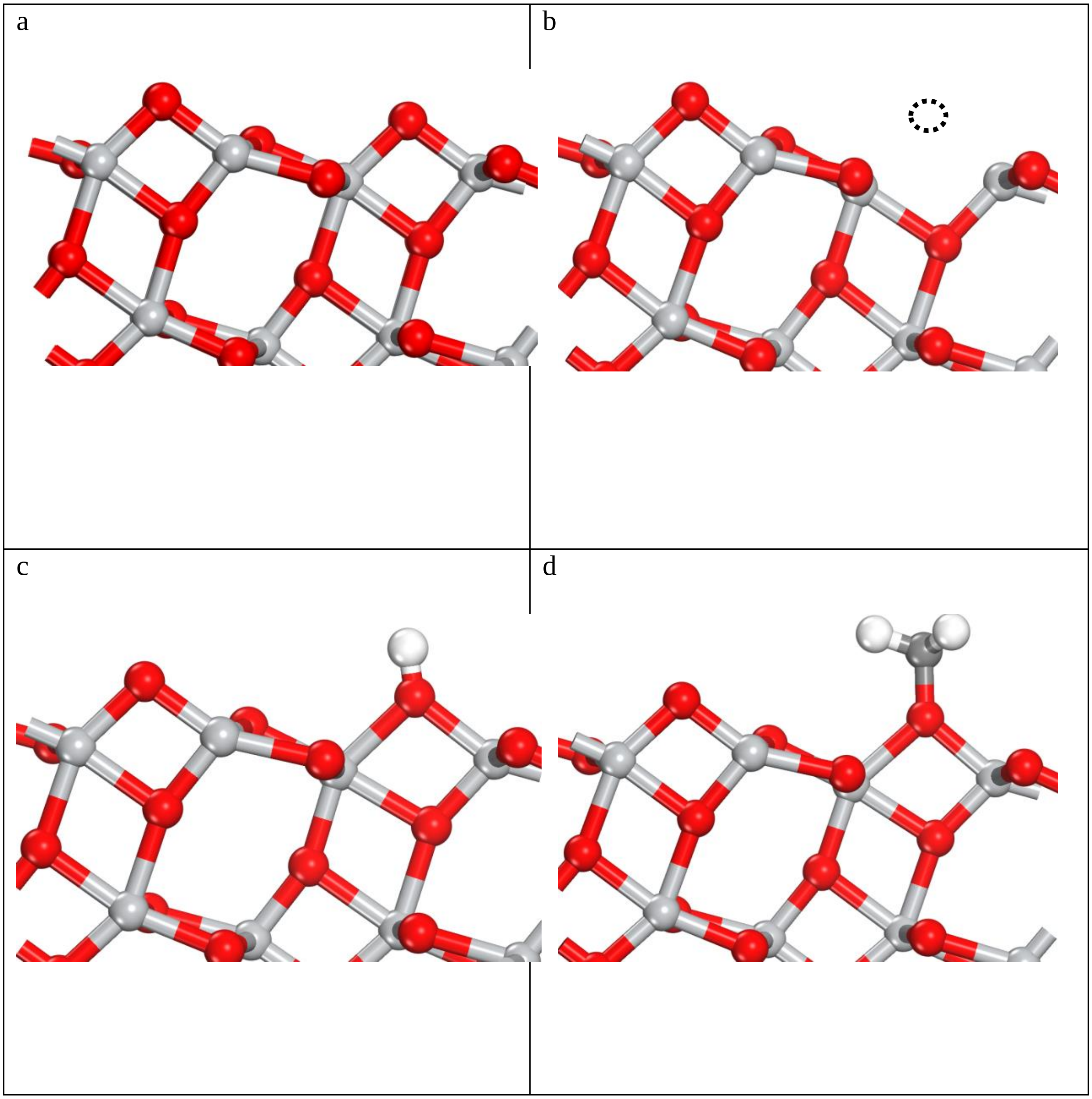

Side views of anatase TiO_2 (101) a) bare surface, b) oxygen vacant surface in the plane (missing oxygen is shown as a dotted circle), with c) H adsorbed at the in-planed oxygen, and d) $\cdot CH_3$ adsorbed at the in-planed oxygen. Ti is shown in grey (light), O is shown in red (dark), C in dark grey, and H in white.

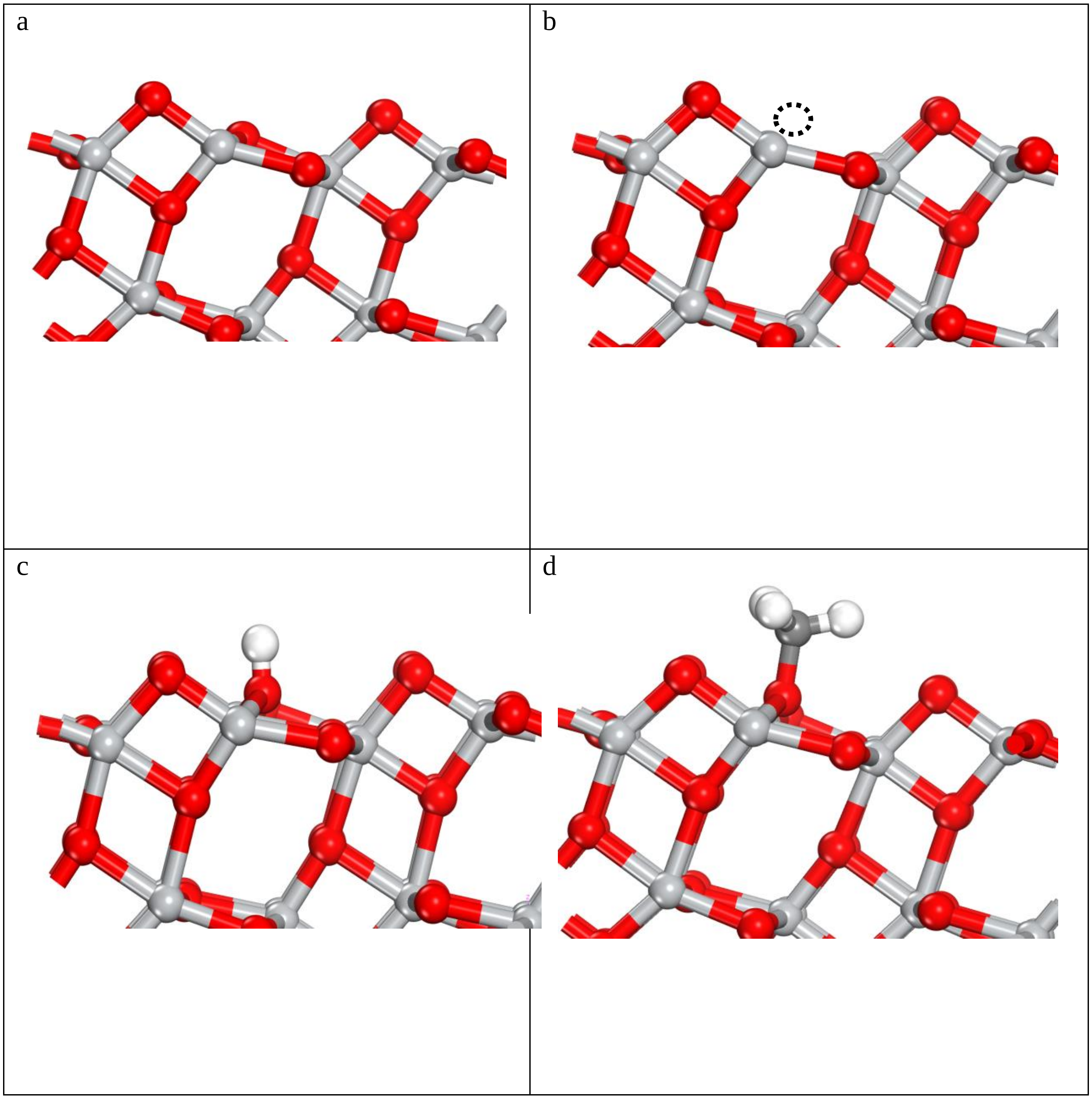

Side views of Ce doped anatase TiO_2 (001) a) bare surface, b) oxygen vacant surface (missing oxygen is shown as a dotted circle), with c) H adsorbed, and d) $\cdot CH_3$ adsorbed. Ce is shown in off white (light), Ti is shown in grey (light), O is shown in red (dark), C in dark grey, and H in white.

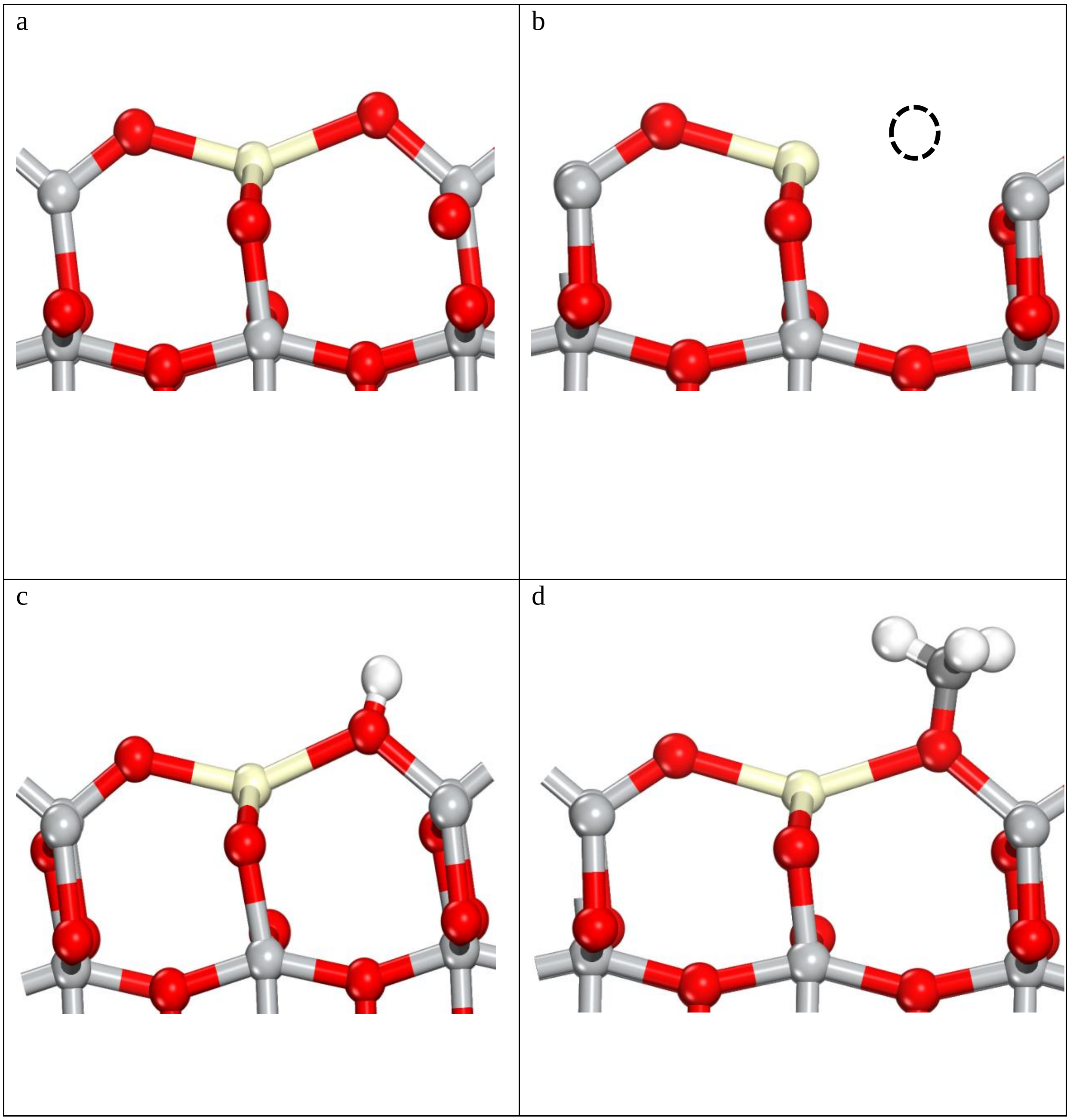

Side views of Ag doped CeO_2 (111) a) bare surface, b) oxygen vacant surface (missing oxygen is shown as a dotted circle), with c) H adsorbed, and d) $\cdot CH_3$ adsorbed. Ag is shown in purple (light), Ce is shown in off white (light), O is shown in red (dark), C in dark grey, and H in white.

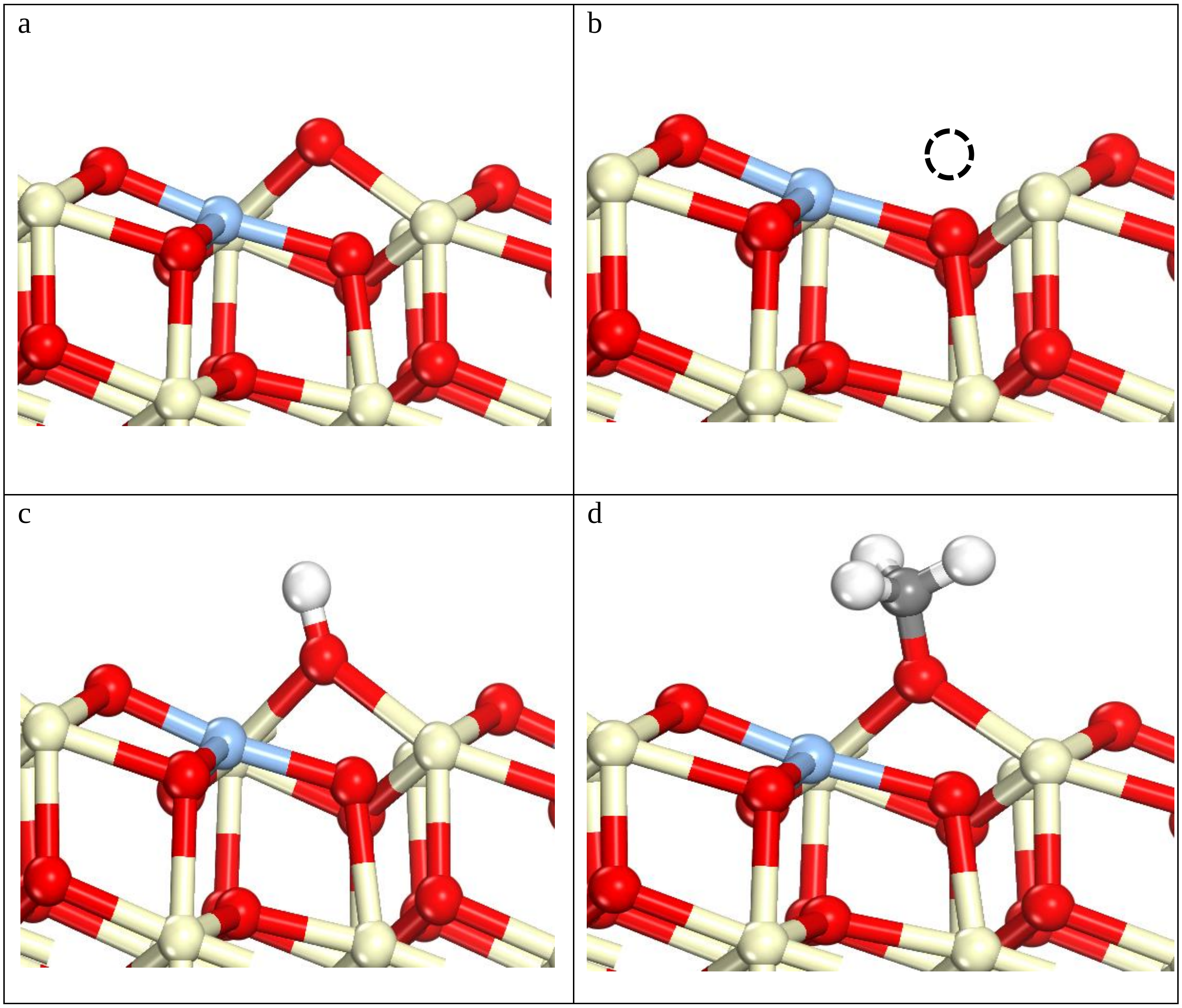

Side views of MgO (110) a) bare surface, b) oxygen vacant surface (missing oxygen is shown as a dotted circle), with c) H adsorbed, and d) $\cdot CH_3$ adsorbed. Mg is shown in green (light), O is shown in red (dark), C in dark grey, and H in white.

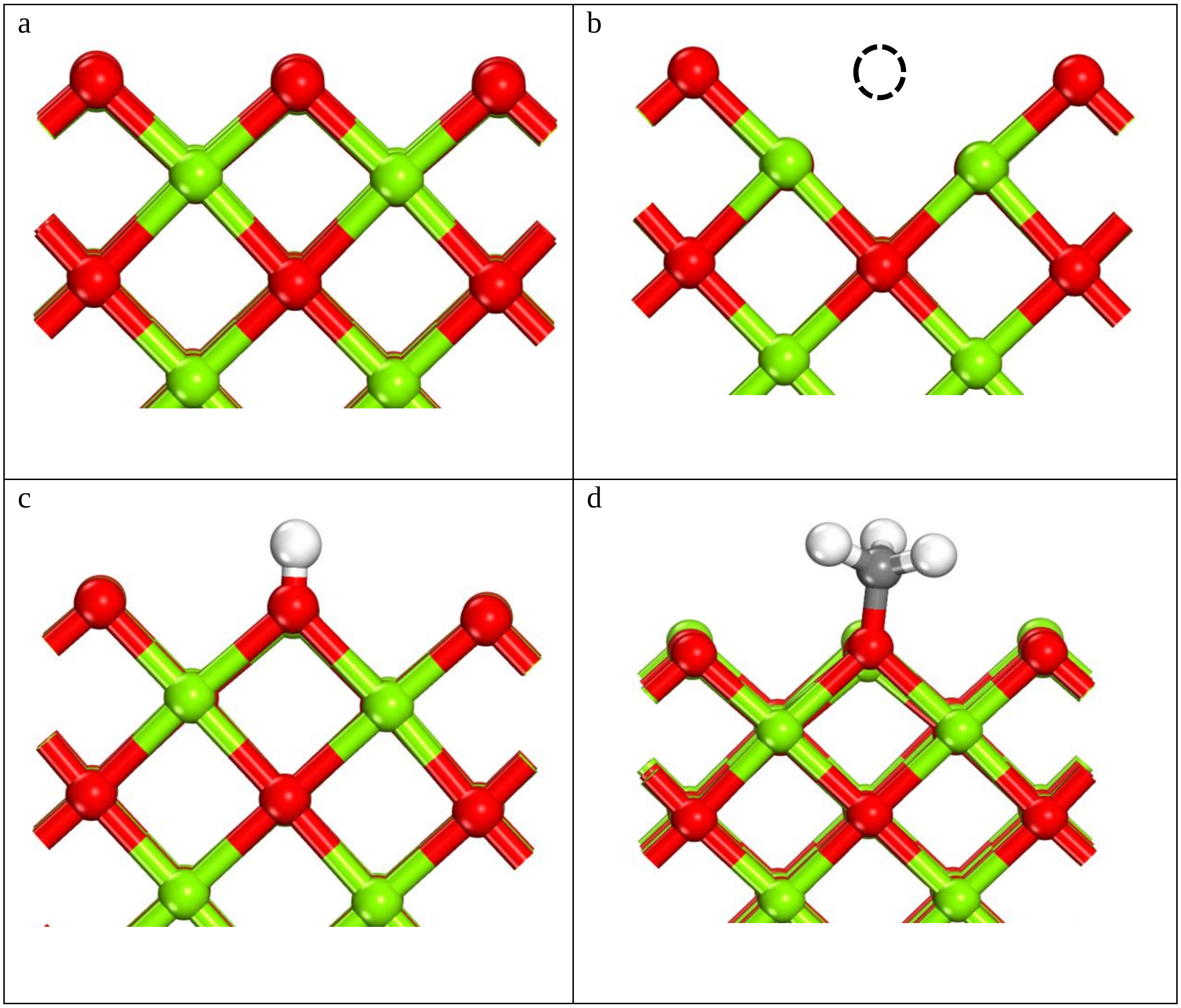

Top view of Pd doped MgO (100) a) bare surface. Side views of Pd doped MgO (100) surface with b) oxygen vacant surface (missing oxygen is shown as a dotted circle), c) H adsorbed, and d) $\cdot CH_3$ adsorbed. Pd is shown in blue (grey), Mg is shown in green (light), O is shown in red (dark), C in dark grey, and H in white.

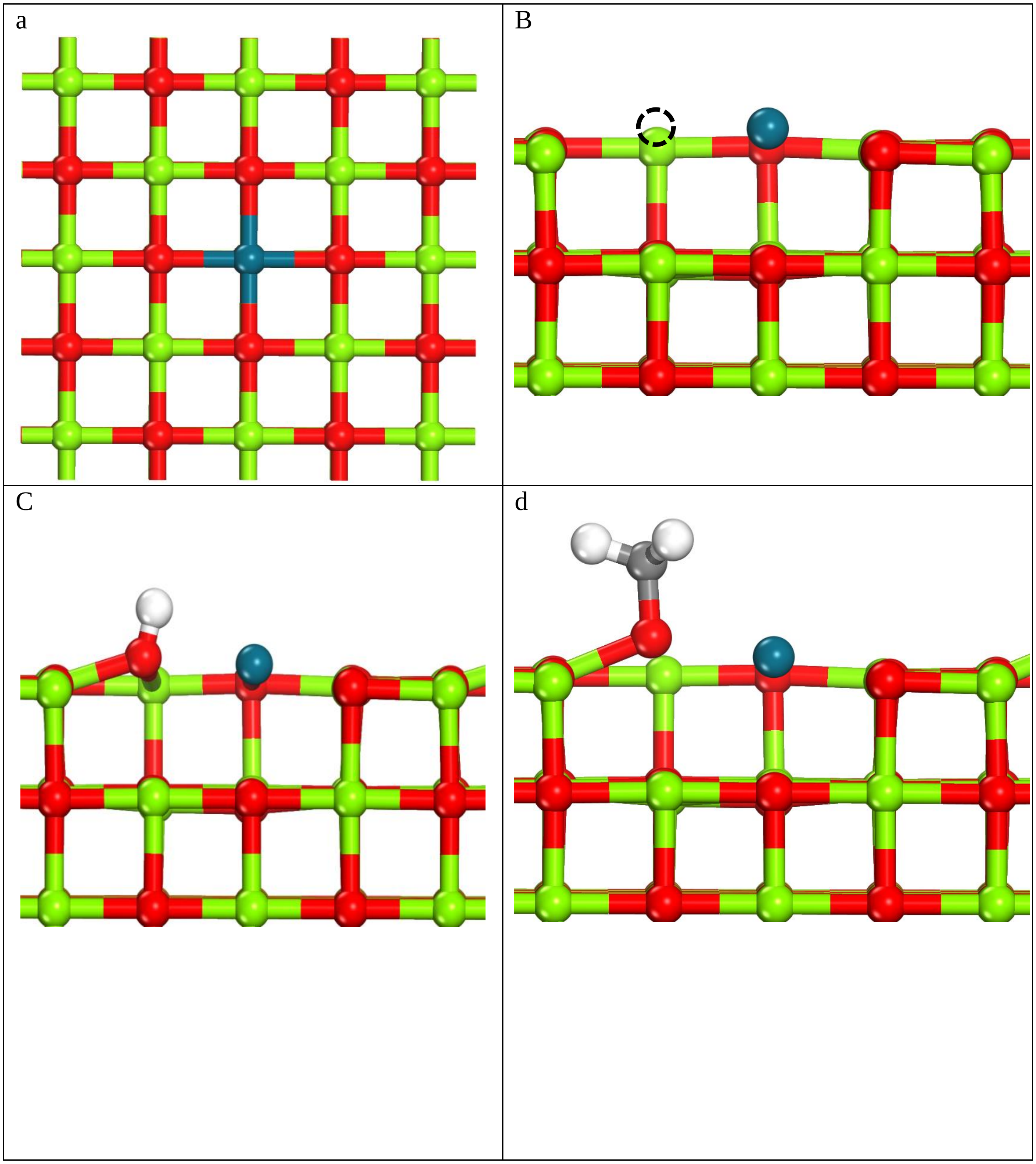

Side views of rutile TiO_2 (110) a) bare surface, b) oxygen vacant surface at the bridge (missing oxygen is shown as a dotted circle), with c) H adsorbed at the bridging oxygen, and d) $\cdot CH_3$ adsorbed at the bridging oxygen. Ti is shown in grey (light), O is shown in red (dark), C in dark grey, and H in white.

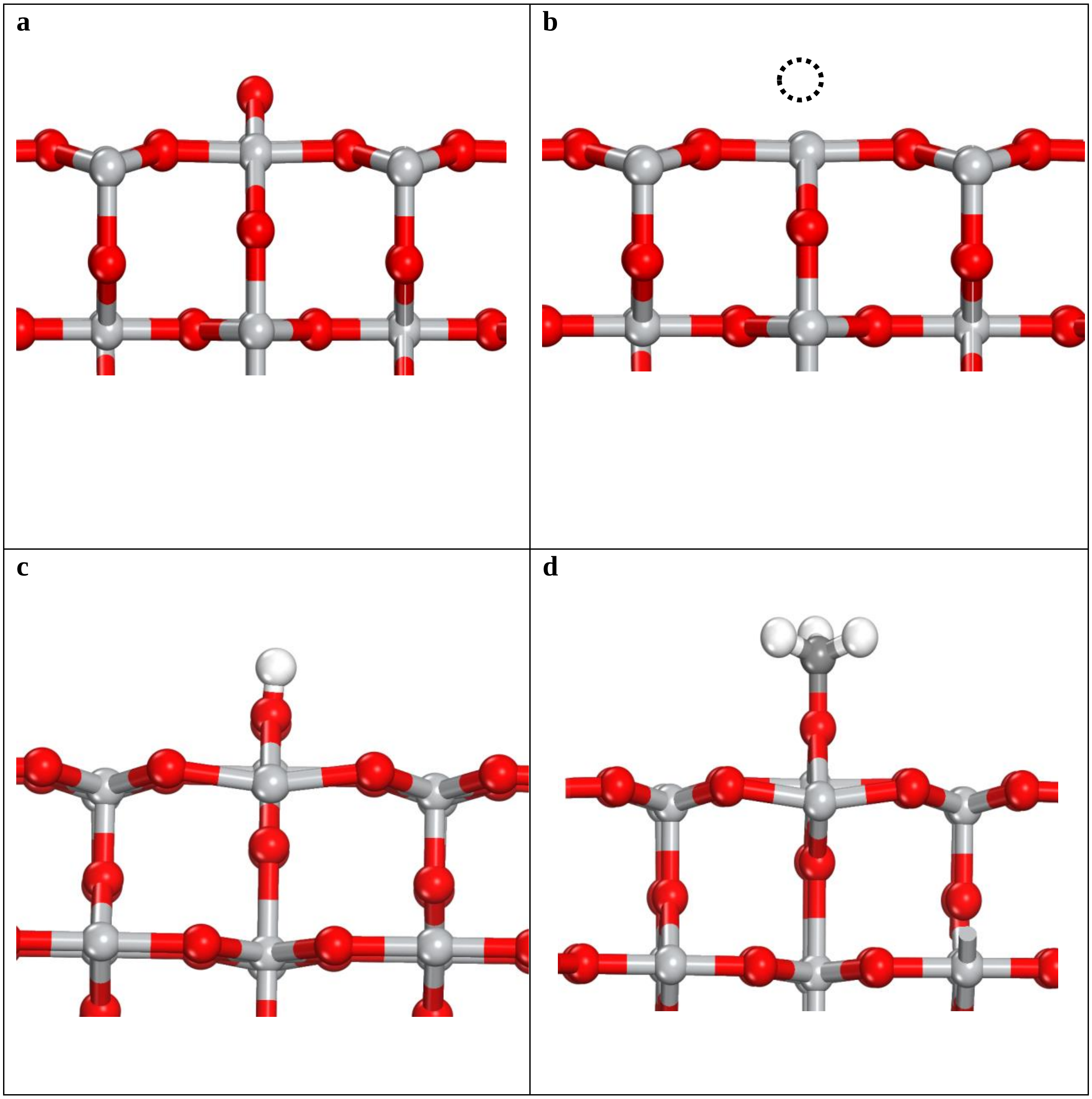

Side views of TbO_2 (111) a) bare surface, b) oxygen vacant surface (missing oxygen is shown as a dotted circle), with c) H adsorbed, and d) $\cdot CH_3$ adsorbed. Tb is shown in green (light), O is shown in red (dark), C in dark grey, and H in white.

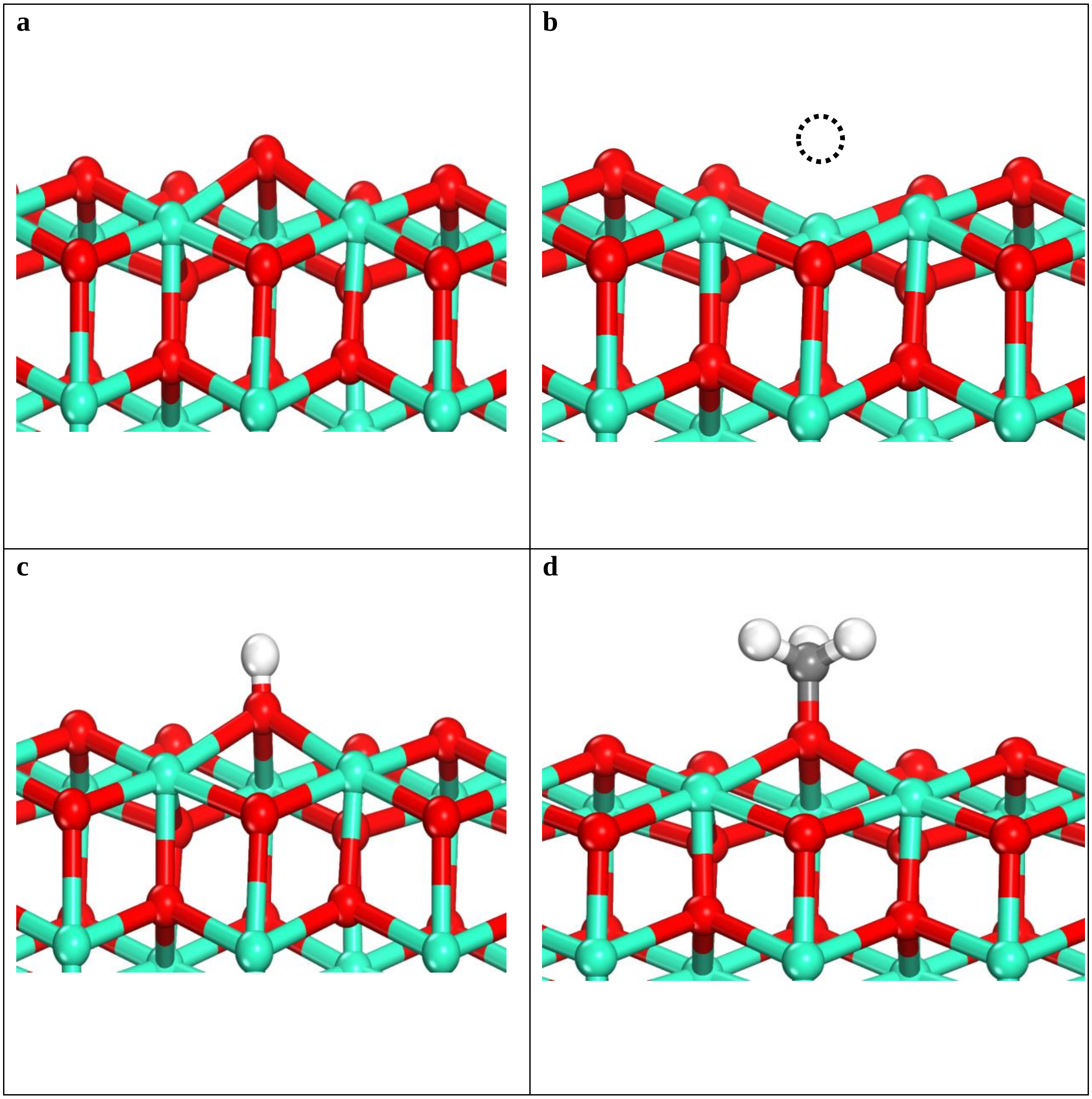

Side views of ZnO (001) a) bare surface, b) oxygen vacant surface (missing oxygen is shown as a dotted circle), with c) H adsorbed, and d) $\cdot CH_3$ adsorbed. Zn is shown as grey (light), O is shown in red (dark), C in dark grey, and H in white.

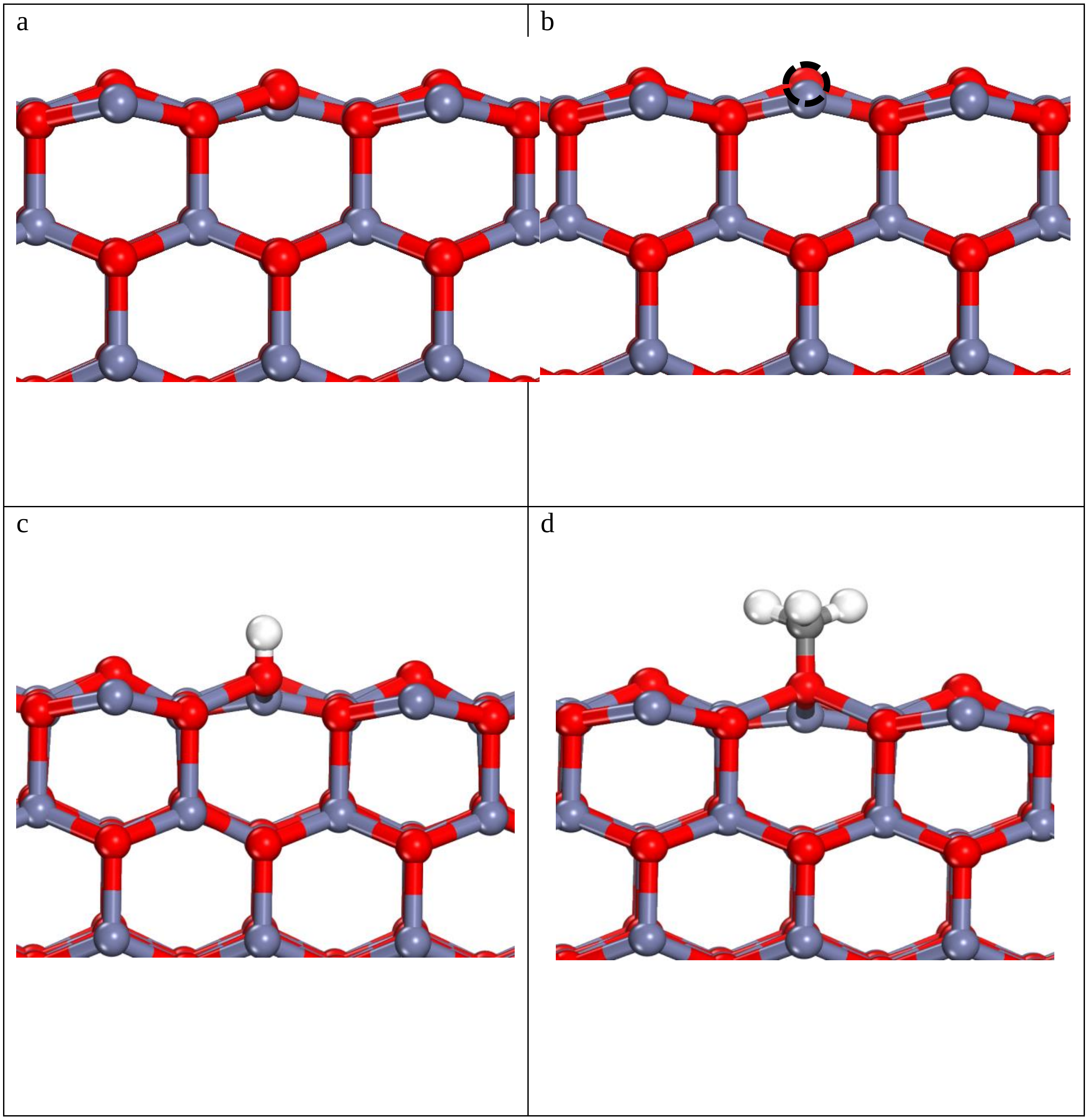

Side views of ZnO (100) a) bare surface, b) oxygen vacant surface (missing oxygen is shown as a dotted circle, with c) H adsorbed, and d) $\cdot CH_3$ adsorbed. Zn is shown as grey (light), O is shown in red (dark), C in dark grey, and H in white.

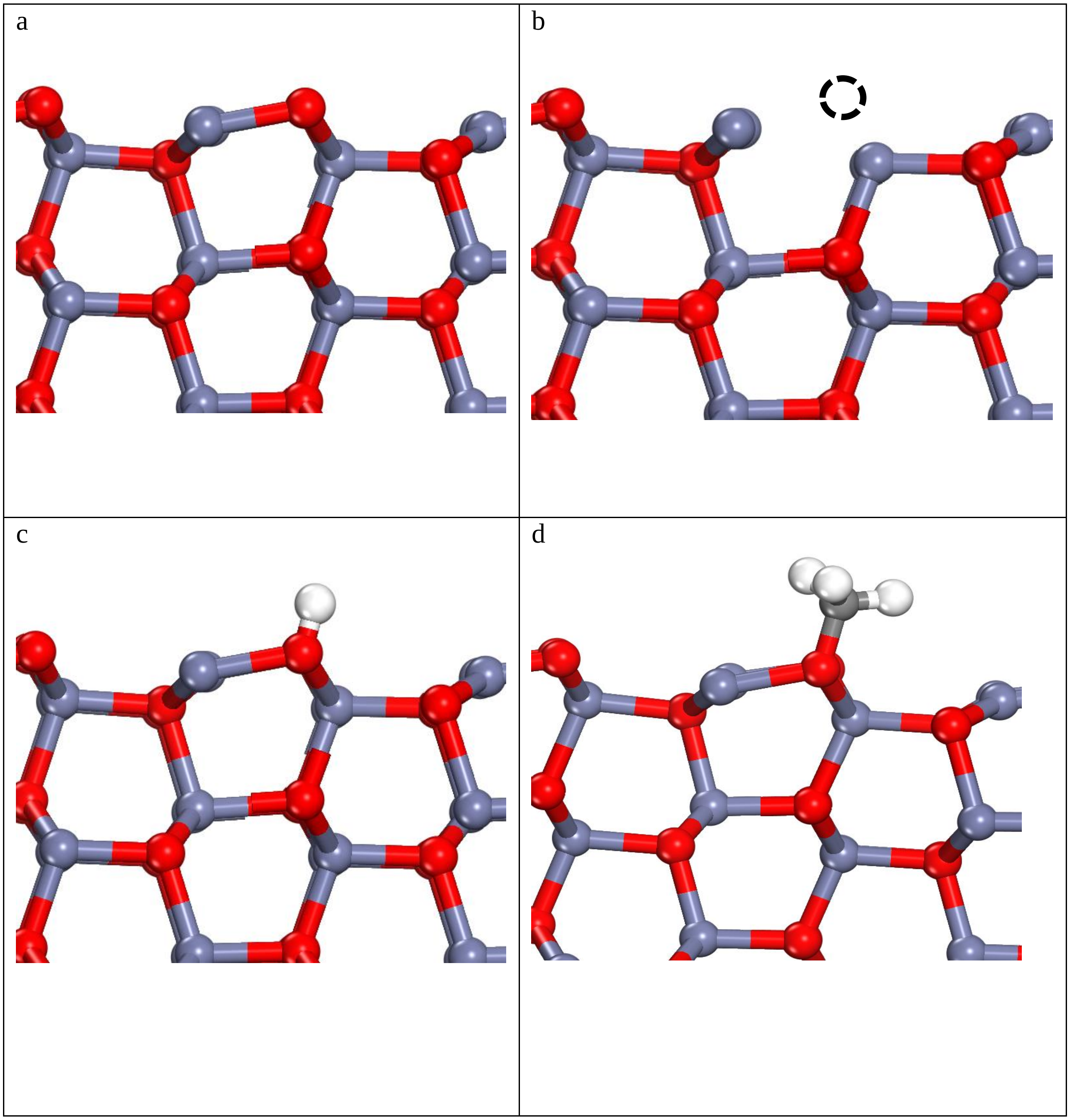

Side views of ZnO (110) a) bare surface, b) oxygen vacant surface (missing oxygen is shown as a dotted circle, with c) H adsorbed, and d) $\cdot CH_3$ adsorbed. Zn is shown as grey (light), O is shown in red (dark), C in dark grey, and H in white.

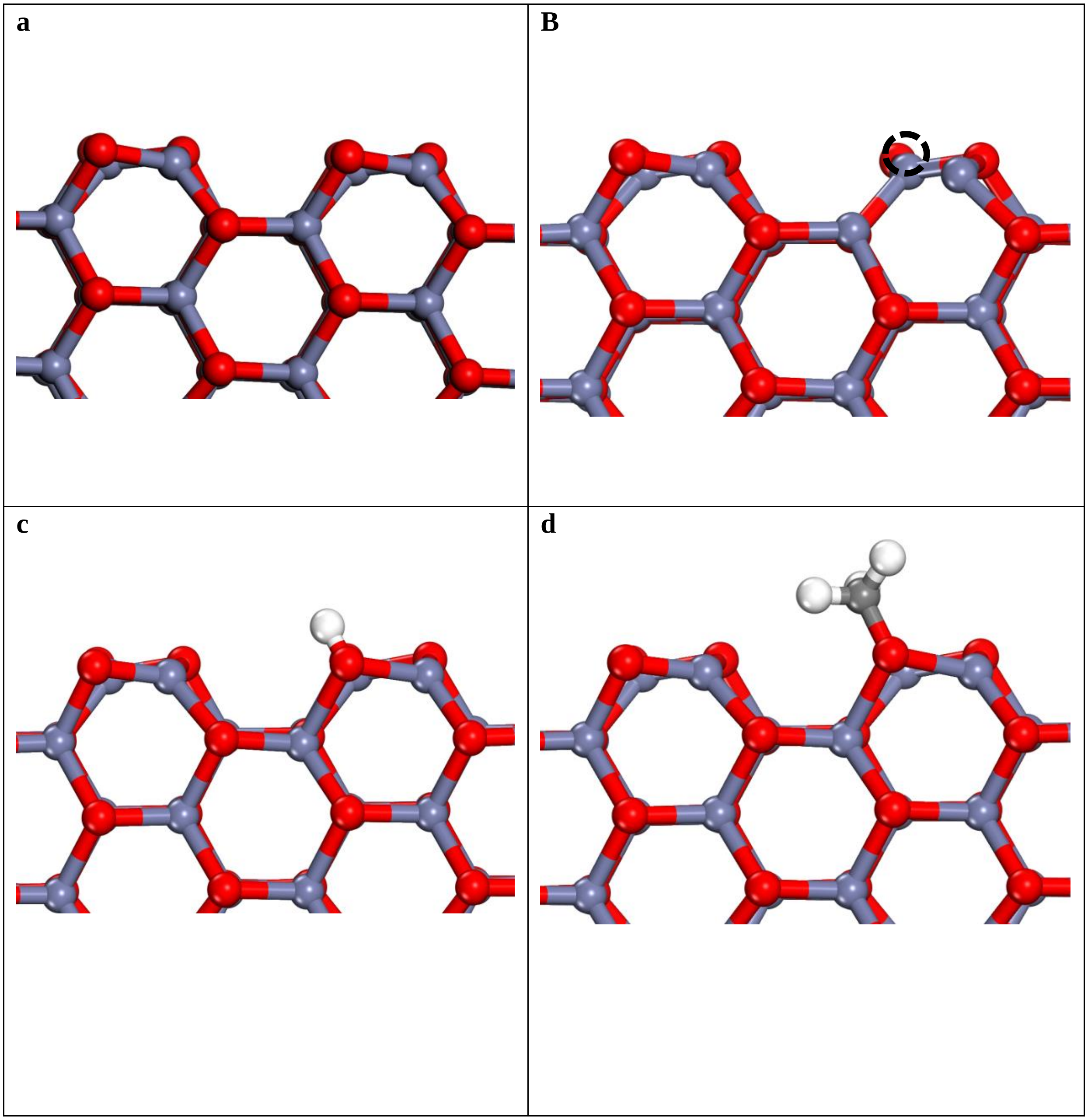

Table S4. Values for Fermi energy, energy in the vacuum and work function

Metal oxide		Fermi energy, E_f (eV)	Energy in vacuum, E_v (eV)	Work function, Φ (eV)
Host oxide	Dopants			
CeO_2 (111)	Ag	0.01	5.42	5.41
	Mn	0.68	5.55	4.87
	Ni	0.41	5.74	5.33
	Pd	0.15	5.43	5.28
	Pt	0.22	5.66	5.44
	V	0.49	5.8	5.32
	W	0.98	4.98	4.00
	Zn	-0.63	5.73	6.35
	Zr	1.29	5.33	4.03
	No dopant	0.53	4.76	4.23
MgO (100)	Be	1.55	4.8	3.25
	Cu	1.37	4.67	3.25
	Ga	1.63	4.77	3.23
	Ge	1.53	4.76	2.59
	Pd	0.87	4.77	3.90
	No dopant	1.39	4.78	3.39
$Tb_{16}O_{32}$		-2.20	3.74	5.95
$Tb_{16}O_{30}$		-2.04	3.56	5.59
$Tb_{16}O_{28}$		-2.08	3.48	5.57
$Tb_{16}O_{26}$		-1.52	3.11	4.63
$Tb_{16}O_{24}$		0.77	3.61	2.85
$Tb_{16}O_{22}$		0.66	3.20	2.54

Table S5. Oxygen vacancy formation energy ΔE_{vac}, C-H activation reaction energy ΔE_{act}, $\cdot CH_3$ adsorption energy ΔE_{ads} of all the pure/doped oxides used in the universal correlation

Metal oxide		Oxygen vacancy formation energy, ΔE_{vac} (eV)	C-H activation reaction energy, ΔE_{act} (eV)	$\cdot CH_3$ adsorption energy, ΔE_{ads} (eV)
Host oxide	Dopant			
CeO_2 (111)	Ag	-0.35	0.23	-3.71
	Mn	0.68	0.15	-3.11
	Ni	-0.10	-0.61	-4.16
	Pd	0.59	0.72	-3.07
	Pt	0.47	0.86	-2.94
	V	1.23	0.74	-2.94
	W	1.93	1.53	-2.33
	Zn	-1.13	-0.21	-4.02
	Zr	1.63	1.10	-2.72
	U-value = 0	3.40	1.81	-1.93
	U-value = 1	3.45	1.85	-1.89
	U-value = 2	3.39	1.84	-1.90
	U-value = 3	3.45	1.74	-1.93
	U-value = 4	3.08	1.70	-2.11
	U-value = 5	2.76	1.29	-2.34
	U-value = 6	2.45	1.13	-2.57
CeO_2 (110)		2.00	0.96	-2.46
MgO (100)	No dopant	6.28	4.37	1.07
	Be	5.89	3.66	0.27
	Cr	5.99	4.45	1.09
	Cu	4.82	2.50	-0.97
	Eu	6.08	4.13	0.78
	Fe	5.73	3.9	0.56
	Ga	5.28	2.47	-0.83
	Ge	5.92	3.56	0.49
	In	5.03	2.43	-0.94
	Li	3.39	0.50	-3.11
	Li$^{\#}$	5.43	3.09	-0.45
	Li*	5.72	2.73	-0.32
	Mn	5.92	4.30	0.86
	Ni	5.31	3.09	-0.39
	Pd	4.23	2.95	-0.63
MgO (110)		5.24	2.99	-0.58
ZnO (001)		3.28	2.48	-1.20
ZnO(100)		2.98	2.30	-1.40
ZnO (110)		2.81	2.44	-1.27

TiO_2	Ana 001	4.08	2.37	-1.37
	Ana100 (brg)	4.76	2.59	-1.34
	Ana100 (ip)	5.46	3.10	-0.73
	Ana101 (brg)	4.88	2.78	-1.14
	Ana101 (ip)	5.45	3.18	-0.59
	Ce	3.88	1.19	-2.56
	Fe	1.63	0.63	-3.06
	Fe and Ce	1.39	0.97	-2.99
	Rut 110 (brg)	2.00	1.05	-2.86
	Zr	5.05	2.59	-0.79
TbO_2		-1.10	-0.20	-3.89
$TbO_{1.88}$		-0.56	-0.18	-3.78
$TbO_{1.75}$		-0.70	-0.04	-3.74
$TbO_{1.63}$		-0.21	0.08	-3.62
$TbO_{1.5}$		5.75	2.95	-0.72
$TbO_{1.38}$		6.39	4.19	0.64

#,* In these cases, 2 Mg atoms have been replaced by 2 Li atoms and one oxygen vacancy has been created to account for the loss of electrons. The calculations over a non-mirrored MgO (100) surface have then been performed over different surface oxygens (# and *), and therefore, the second oxygen vacancy formation has been used as the surface reducibility descriptor.

brg represents the surface where the bridging oxygen is removed to represent the oxygen vacancy formation, while ip represents the vacancy formation of the in surface place oxygen.

Table S6. Statistical details of the correlation between C-H bond activation of methane ΔE_{act} and the oxygen vacancy formation energy ΔE_{vac}, and the -·CH_3 adsorption energy ΔE_{ads} and the oxygen vacancy formation energy ΔE_{vac}

Linear regression analysis on predictor y using response x:
Model: y = Ax + B

Data	y	x	A	B	R^2	95% CI	
						A	B
Overall	ΔE_{act}	ΔE_{vac}	0.569	0.081	0.88	0.510, 0.629	-0.157, 0.320
	$-\Delta E_{ads}$	ΔE_{vac}	-0.616	3.687	0.88	-0.681, -0.552	3.430, 3.945
CeO_2 U value	ΔE_{act}	ΔE_{vac}	0.703	-0.584	0.95	0.508, 0.897	-1.199, 0.032
	$-\Delta E_{ads}$	ΔE_{vac}	-0.664	4.179	0.99	-0.737, -0.591	3.950, 4.409
TiO_2 facet	ΔE_{act}	ΔE_{vac}	0.595	-0.131	0.99	0.525, 0.666	-0.457, 0.195
	$-\Delta E_{ads}$	ΔE_{vac}	-0.614	4.063	0.97	-0.764, -0.463	3.371, 4.755
TbO_x	ΔE_{act}	ΔE_{vac}	0.548	0.259	0.97	0.429, 0.667	-0.165, 0.682
	$-\Delta E_{ads}$	ΔE_{vac}	-0.557	3.407	0.97	-0.688, -0.426	2.942, 3.873

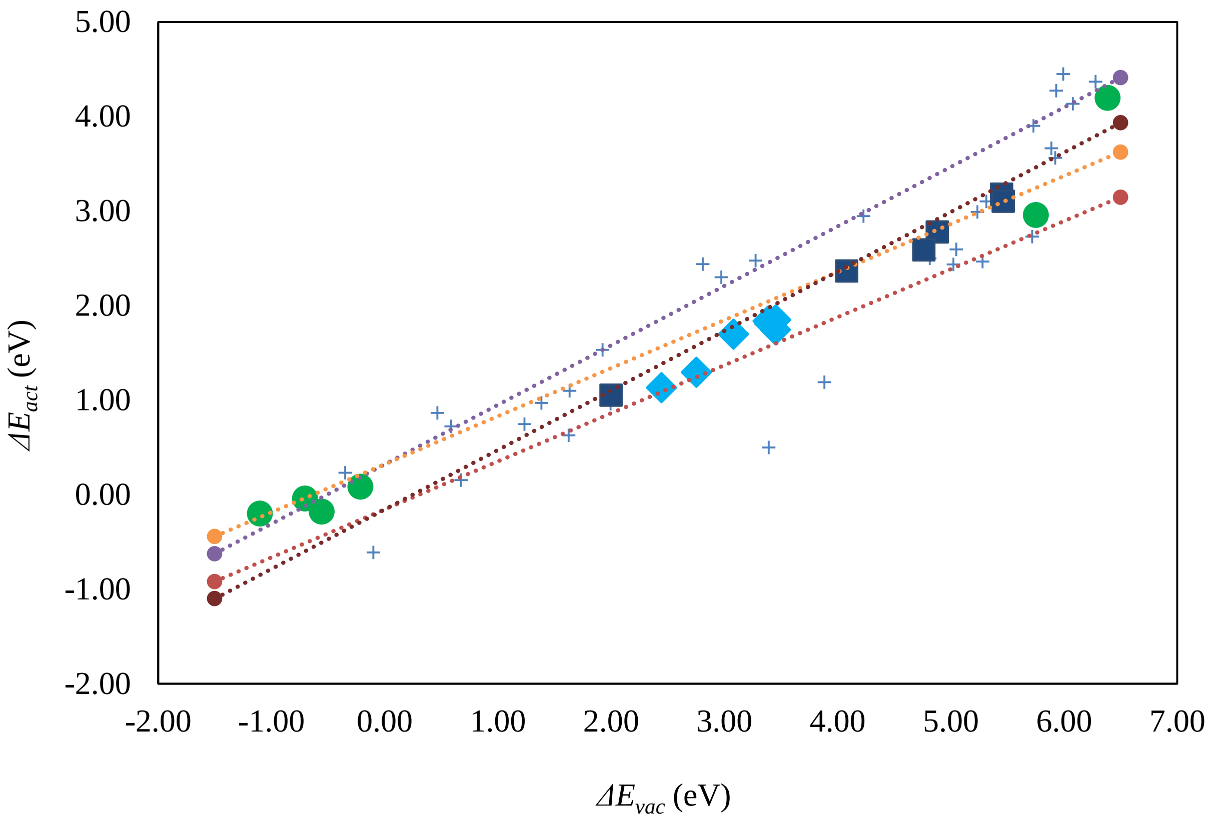

Here, the four dotted lines represent the regression lines with 95% CI coefficients, A and B. All the sub-correlations: varying the U-value for Ce in CeO_2 (◆), the surface facets for TiO_2 (■) and the oxidation state for TbO_x (●) lie within this confidence interval.

Table S7. The position of oxygen vacancies in various stable oxidation states of TbO_x in a mirrored $Tb_{16}O_{32}$ surface slab

TbO_x	Stoichiometry	Vacancy				Total number of oxygen vacancies*
		Top	Sub1	Sub2	Sub3	
TbO_2	$Tb_{16}O_{32}$	0	0	0	0	0
$TbO_{1.88}$	$Tb_{16}O_{30}$	0	0	1	0	2
$TbO_{1.75}$	$Tb_{16}O_{28}$	1	0	1	0	4
$TbO_{1.63}$	$Tb_{16}O_{26}$	2	0	1	0	6
$TbO_{1.5}$	$Tb_{16}O_{24}$	2	0	2	0	8
$TbO_{1.38}$	$Tb_{16}O_{22}$	4	0	1	0	10

*Since we use a mirrored surface, total number of oxygen vacancies is twice the number of vacancies in a particular surface layer.